Appl. Phys. B (2013) 113:99–106
DOI 10.1007/s00340-013-5444-z

Applied Physics B
Lasers and Optics

Crystal growth and characterization of a novel inorganic–organic hybrid NLO crystal: $(NH_4)[Cd(NCS)_3]\cdot C_{12}H_{24}O_6$

V. Ramesh · K. Rajarajan

Received: 4 December 2012 / Accepted: 6 April 2013 / Published online: 10 May 2013

Abstract It is reported here, for the first time, that high-quality bulk size ($18 \times 5 \times 4$ mm^3) single crystals of a new nonlinear optical crystal, $[(NH_4)[Cd(NCS)_3]\cdot C_{12}H_{24}O_6]$ [Ammonium (18-crown-6-ether) Cadmium(II) tri-thiocyanate; ACCTC], have been grown from aqueous solution via slow evaporation technique. Solubility of ACCTC has been determined for various temperatures. The grown crystals were characterized by single crystal X-ray diffraction, FT-IR, FT-Raman, and UV–Vis–NIR studies. ACCTC crystallizes in orthorhombic system with cell parameters $a = 14.7568$ Å, $b = 15.4378$ Å, and $c = 10.6383$ Å with space group $Cmc2_1$. The optical second-harmonic generation effect has been measured by using the Kurtz powder technique and is found to be 2 times higher than that of KDP (KH_2PO_4). The sample possesses wide optical transparency range from 200 to 2,500 nm. The TG-DSC thermal analysis revealed that the sample is thermally stable up to 237.92 °C, which is comparatively far better than the thermal stability of [(18C6)Li][Cd(SCN)$_3$]; CLTC (170 °C).

1 Introduction

Very recently, the nonlinear optical crystals for second-harmonic generation (SHG) have received much attention as they play a vital role in the field of telecommunications, optical computing, optical information processing, optical data storage, laser remote sensing, laser driven function, and color displays. In photonics, a growing need continues for low cost, highly nonlinear efficient, and high-quality crystals for optical frequency conversion [1–5]. Inorganic materials exhibit high melting point, high mechanical strength, and high degree of chemical inertness in spite of their poor optical transparency. Organic materials are often formed by weak Van der Waal and hydrogen bonds and possess a high degree of delocalization. Some of the advantages of organic materials include flexibility in the methods of synthesis, high nonlinearity, and high damage resistance, etc. However, organic compounds have weak thermal and mechanical stability. The inherent limitations of both inorganic and organic crystalline materials have led researchers to find alternate strategies. The obvious one was to combine the superior qualities of both inorganic and organic materials in the same compound.

Among the inorganic–organic compounds, it is interesting to note that the metal-thiocyanate complex family crystalline compounds offer a variety of molecular structures by virtue of the changes brought out in selection of metals, ligands, coordination numbers, and so on. These complexes are capable of efficient frequency conversion of infrared laser radiation into visible and ultraviolet wavelengths and are developed on the basis of the molecular engineering method and the double-ligand model. In metal-thiocyanate complexes, the thiocyanate (SCN) plays a crucial role in combining the versatile ambidentate ligand with two donor atoms. It can coordinate through either the nitrogen or the sulfur atom, or both, giving rise to linkage isomers or polymers [6–17]. Recently, inorganic polymers with organic spacers (IPOS) hybrid system have received renewed attention, as it combines the superior qualities of both inorganic, organic, and polymer materials. In IPOS series, thiocyanate (SCN) ligand forms a coordination

V. Ramesh
Research and Development Centre, Bharathiar University, Coimbatore 641 046, India

K. Rajarajan (✉)
Department of Physics, Rajeswari Vedachalam Government Arts College, Chengalpet 603 001, Tamil Nadu, India
e-mail: drkrr2007@gmail.com

polymeric chain combined with the d^{10} transition metal ion and leads a noncentrosymmetric structure. It is a new class of series of coordination solids described as IPOS with the general formula [H–G][M–L], where the inorganic anion $[M–L]^-$ is metal (M)–ligand (L) coordination polymer such as $[Cd(SCN)_3]^{\infty}$ and the organic cation $[H–G]^+$ is a host (H)–guest (G) complex such as [(crown ether)–(alkali metal)]. These IPOS coordination solids form a wide variety of structures, ranging from one-dimensional chain to two-dimensional-layered structures depending upon the size, shape, symmetry, and charge of the cationic host–guest complexes [18–21]. Earlier, Zhang and Zelmon [22] have reported the growth of a new hybrid nonlinear optical compound [(18C6)K][Cd(SCN)$_3$], which is optically transparent from 220 to 3,300 nm and exhibits efficient SHG. Recently, Zhang and Shu [23] and Zhang and Huang [24] have reported the growth and characterization aspects and powder SHG of [(18C6)Li][Cd(SCN)$_3$], respectively. In the present work, a new nonlinear optical crystalline compound $[(NH_4)[Cd(NCS)_3]\cdot C_{12}H_{24}O_6]$ [Ammonium (18-crown-6-ether) Cadmium(II) tri-thiocyanate; ACCTC] has been synthesized, and single crystals of ACCTC with dimension of 18 × 5 × 4 mm^3 were grown from aqueous solution via slow evaporation technique for the first time. Earlier, the crystal structure of ACCTC was determined and reported by our research group (IUCr Ref. ZB2021) [25]. This compound crystallizes in an orthorhombic crystal system of space group $Cmc2_1$ with cell parameter $a = 14.7568$ Å, $b = 15.4378$ Å, $c = 10.6383$ Å, $V = 2423.54$ (18) Å^3, and $Z = 4$. For SHG, it is very important to arrange the anionic chains in a parallel fashion in order to attain a noncentrosymmetric crystal structure. Our work in this area led to the discovery of a new series of hybrid NLO crystal based on polymeric cadmium-thiocyanate anions and cations. It is interesting to note that $[(NH_4)[Cd(NCS)_3]\cdot C_{12}H_{24}O_6]$ (ACCTC) is a highly efficient SHG crystalline material whose conversion efficiency is about 2 times superior to KDP. In the present compound, the parallel arrangement of the anionic $[Cd(NCS)_3]$ zig-zag chains results in the noncentrosymmetric structure. As a result, it possesses nonlinear optical property. In the present work, we are reporting the synthesis, growth, optical, thermal, and nonlinear optical properties of ACCTC for the first time.

2 Experimental section

2.1 Material synthesis

The starting materials were used as commercially available analytical-grade reagents. The title compound was prepared as per the following equation.

$$C_{12}H_{24}O_6 + CdCl_2 + 3(NH_4SCN) \rightarrow [(NH_4)[Cd(NCS)_3]\cdot C_{12}H_{24}O_6] + 2NH_4Cl$$

The calculated amounts of salts were dissolved in deionized water at room temperature. The mixture was filtered, and the resulting colorless solution was kept for slow evaporation. Initially, the small millimeter seed crystals started growing from surface of liquid. Colorless, transparent, seed crystals of ACCTC were collected after 15–20 days (Fig. 1). The purity of the synthesized compound was improved by successive recrystallization process.

2.2 Solubility studies

The growth rate of a crystal depends on its solubility and temperature. The solubility test of ACCTC was performed in an aqueous solution in the temperature range 30–60 °C. Initially, a 250-ml capacity glass beaker containing 100 ml of aqueous solution was placed in the temperature bath and the temperature was set at 30 °C. The powdered sample of ACCTC was gradually added to the solution in small amount and subsequently stirred by a motorized stirrer till the excess salt was deposited at the bottom of the beaker. The stirring was further continued, to ensure homogeneous temperature and equilibrium concentration throughout the

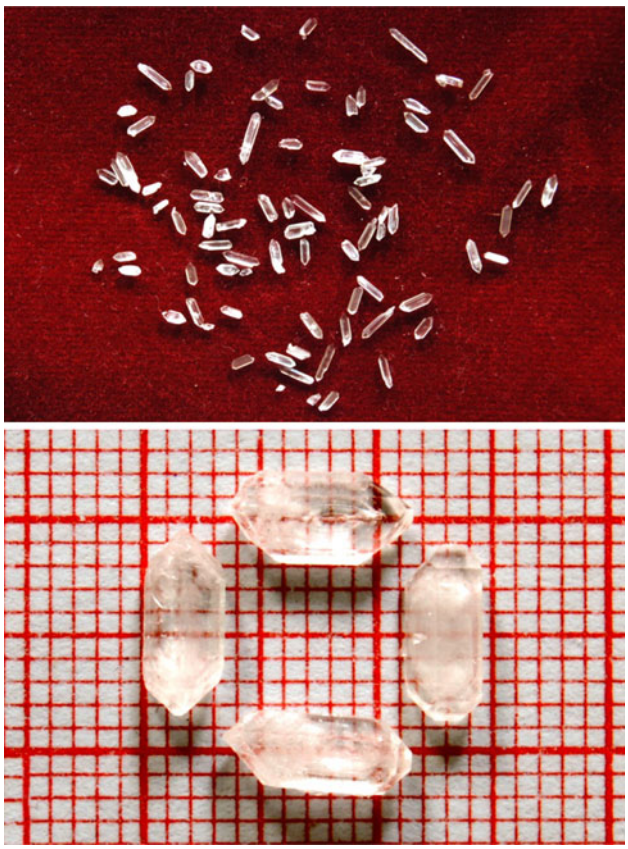

Fig. 1 As grown seed crystals of ACCTC

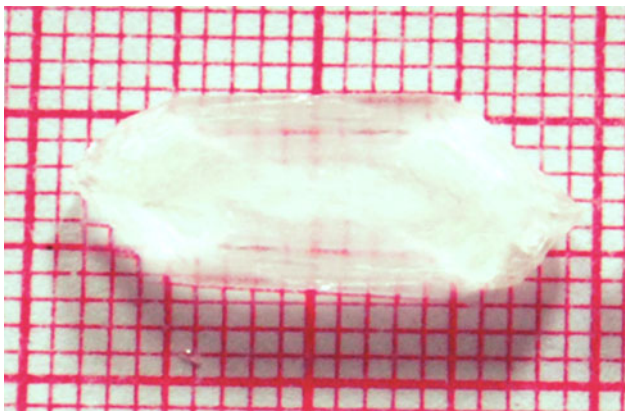

Fig. 2 As grown bulk size ACCTC crystal

entire volume of the solution. After confirming the equilibrium saturation, the content of the solution was analyzed gravimetrically. A 20 ml of the saturated solution of the sample was withdrawn by means of a pipette, and the same was poured into a cleaned, dried, and weighed petri dish. The solution was then kept for slow evaporation in a heating mantle till its complete evaporation. The mass of ACCTC in 20 ml of solution was determined by weighing the petri dish with salt, and hence, the solubility, that is, the quantity of ACCTC salt (in gram) dissolved in 100 ml of mixture solvent was determined. The above procedure was repeated for various temperature intervals up to 60 °C. One of the main problems in the growth of crystals of the IPOS series is their low solubility in water and many organic solvents. Figure 2 depicts the solubility of ACCTC in water as a function of temperature. It is seen that the solubility significantly increases with increasing temperature.

2.3 Bulk growth of ACCTC

To grow centimeter size single crystal of the title compound ACCTC, small millimeter-sized good quality single crystals, grown by spontaneous crystallization at room temperature, were selected as seeds. Two hundred milliliters of the mother solution was prepared and saturated at room temperature and then filtered to remove any impurities. The chosen seed crystal was carefully mounted in the upper level of the saturated solution with suitable arrangement and kept for slow evaporation. Good quality single crystals of dimensions 18 × 5 × 4 mm^3 were obtained over a period of 3 weeks (Fig. 3).

3 Results and discussion

3.1 Single crystal XRD

Single crystal X-ray diffraction (XRD) analysis was carried out on ACCTC using a Bruker Kappa APEXII CCD

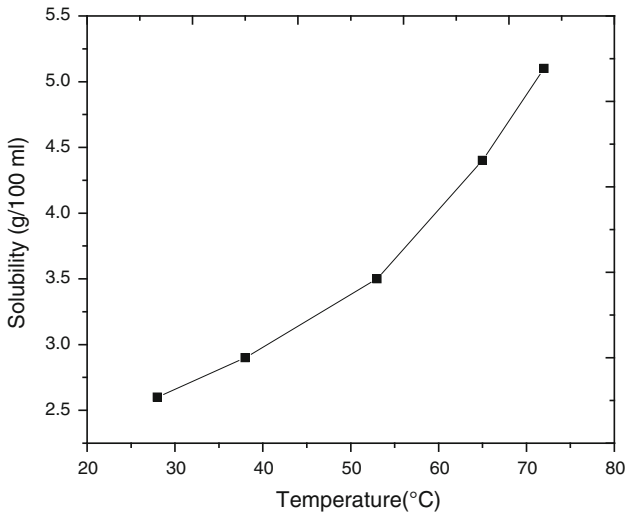

Fig. 3 The solubility of ACCTC crystal in an aqueous solution

Table 1 Crystal data of ACCTC

Emperical formula	$[(NH_4)[Cd(NCS)_3]\cdot C_{12}H_{24}O_6]$
M_r	568.99
Wavelength	0.71073 Å
T	293 K
Crystal system	Orthorhombic
Space group	$Cmc2_1$
Cell dimensions	$a = 14.7568\ (6)$ Å
	$b = 15.4378\ (6)$ Å
	$c = 10.6383\ (5)$ Å
	$V = 2423.54\ (18)$ $Å^3$
Z	4
D_x	1.559 mgm^{-3}

diffractometer with graphite monochromated Mo-Kα radiation ($\lambda = 0.71073$ Å). ACCTC crystallizes in a noncentrosymmetric orthorhombic crystal system with the space group $Cmc2_1$ [25]. The unit cell parameters of ACCTC are presented in Table 1. In ACCTC, the Cd^{2+} ion, the ammonium ion, and SCN^- ligands are located on mirror planes. The thiocyanate anions function as bridging ligands between the Cd_{II} ions, leading to a chain-like arrangement, which are parallel to one another and expanding along [001] direction. The ammonium molecules are contained within the bowl of the macrocycle via extensive N–H–O hydrogen bonding as shown in Figs. 4, 5 and 6. The incorporation of NH_4^+ cation within the cavity of 18-crown-6-ether has already been well established and reported elsewhere [26–28].

3.2 FT-IR studies

The powdered crystal of ACCTC was subjected to BRUKER IFS 66 V FT-IR spectrometer to confirm the presence

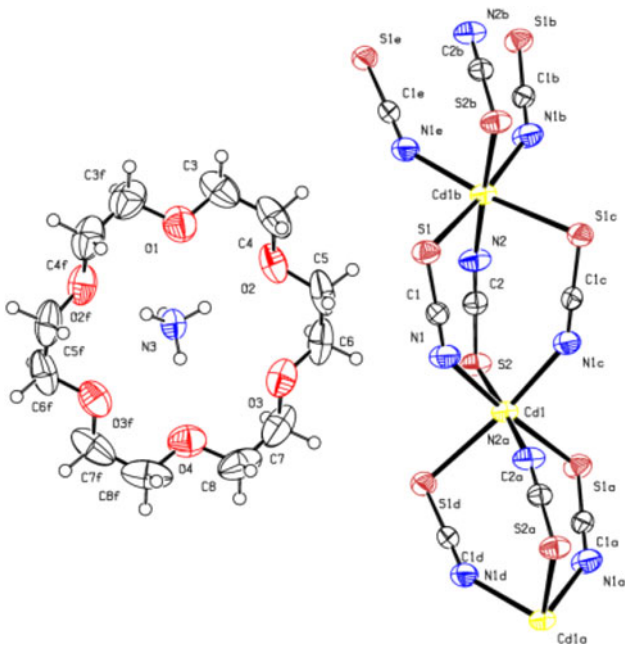

Fig. 4 ORTEP diagram of $[(18C6)NH_4]^+[Cd(SCN)_3]^-$ (50 % probability thermal ellipsoids). H atoms are drawn as small spheres of arbitrary radii

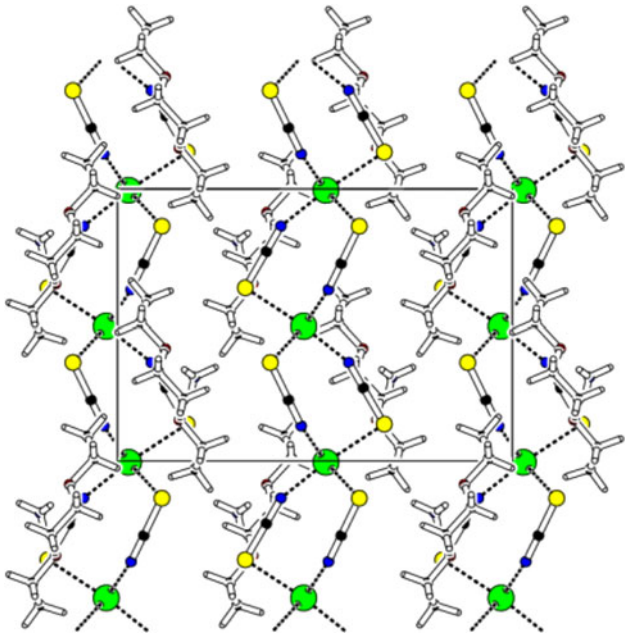

Fig. 5 Crystal packing of $[(18C6)NH_4]^+[Cd(SCN)_3]^-$ as viewed along the crystallographic *a* axis

of functional groups and coordination of ligands in the wavenumber range 400–4,000 cm^{-1} as shown in Fig. 7. The spectral profile of NH_4SCN was shown in Fig. 8 and compared with ACCTC. The IR vibrational frequencies of ACCTC along with NH_4SCN and 18C6 are presented in Table 2. The prominent absorption peaks of ACCTC were

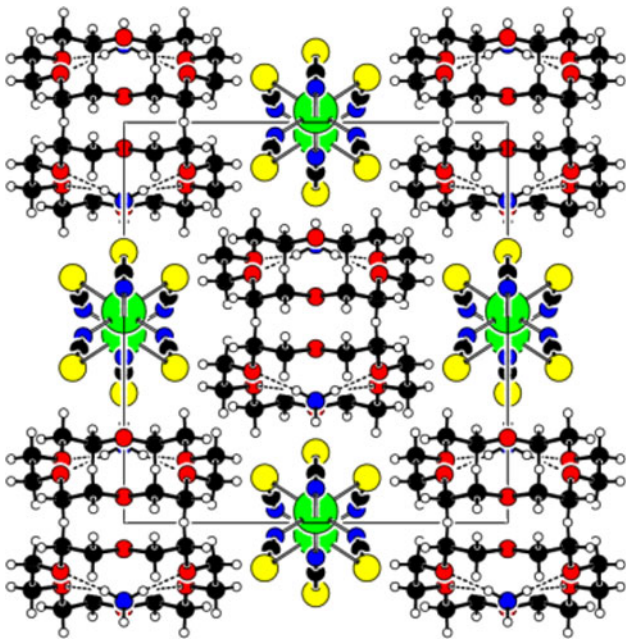

Fig. 6 Crystal packing of $[(18C6)NH_4]^+[Cd(SCN)_3]^-$ as viewed along the crystallographic *c* axis

found to be shifted when compared with pure 18-crown-6-ether. The sharp and intense bands observed at 1107.5 and 956.0 cm^{-1} were shifted from 1,037 and 940 cm^{-1} of pure 18-crown-6-ether, respectively, which is due to asymmetric C–O–C stretching vibration. In addition, the sharp and intense band observed at 1353.2 was shifted from 1,349 cm^{-1} of CLTC [24], which is due to $-CH_2-$ stretching vibration. The CN stretching vibration mode of SCN appears as a very strong and highly intense sharp band at 2120.8 cm^{-1}. Interestingly, the CN stretching vibration of ACCTC (2120.8 cm^{-1}) was shifted from 2048.99 cm^{-1} of pure NH_4SCN. It is worth noting that the NH_4^+ vibration at 3249.5, 3205 cm^{-1} and shift in C–O–C vibration of the crown ether indicate the coordination of the crown ether to the NH_4^+ cation.

3.3 FT-Raman studies

The FT-Raman spectrum of ACCTC was recorded on the powder sample of ACCTC in the range of 50–4,000 cm^{-1} using BRUKER RFS 27 Raman spectrometer, and the recorded spectral profile is shown in Fig. 9. The presence of functional groups of various elements were identified and listed in Table 3. The Raman spectrum clearly shows the bending vibration modes of Cd metal ions at 275.27 and 213.90 cm^{-1}, respectively. These modes confirm the coordination Cd ions with the SCN ligand. In addition, the presence and binding of SCN is strongly influenced as a strong peak observed at 2105.82 cm^{-1}, which corresponds to the CN stretching vibration of SCN. From the structural

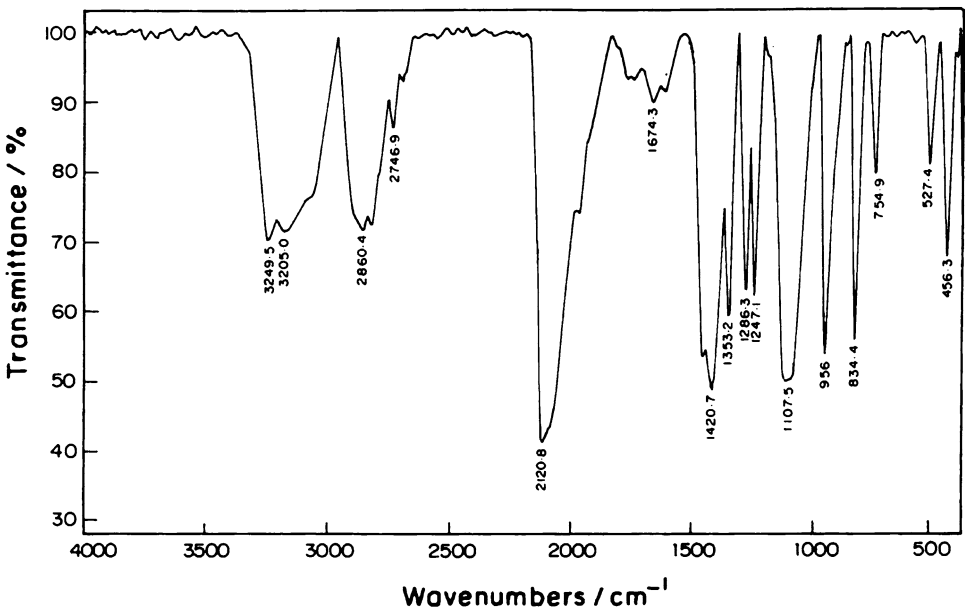

Fig. 7 FT-IR spectrum of ACCTC

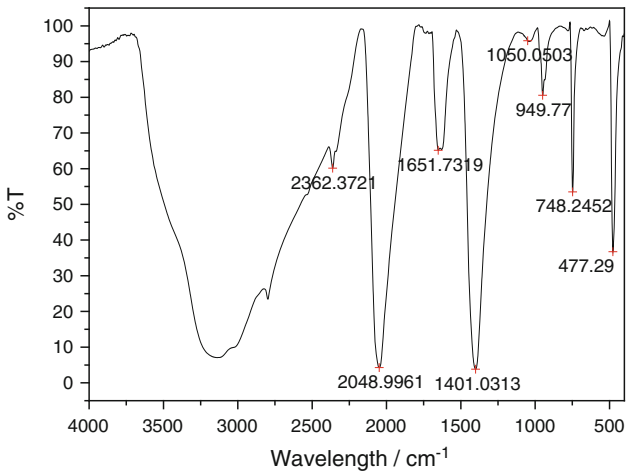

Fig. 8 FT-IR spectrum of NH_4SCN

Table 2 Selected FT-IR spectral assignments of ACCTC in comparison with NH_4SCN and 18C6

Assignments	Wavenumber (cm^{-1})		
	ACCTC	NH_4SCN	18C6
NH stretching vibrations	3249.5, 3205.0, 2860.4	–	–
CN stretching of SCN	2120.8	2048.99	–
CH_2 stretching vibration	1420.7, 1353.2	–	1333.0
Asymmetric C–O–C stretching	1107.5	–	1037.0
Symmetric C–O–C stretching	956.0	–	940.0
Twice NCS bending vibrations	834.49	949.77	–
CS stretching of SCN	754.9	748.24	–
NCS bending vibrations	456.3	477.29	–

point of view (Fig. 2), it is clearly evident that the Cd atoms are octahedrally coordinated with three nitrogen and three sulfur atoms, from six SCN^- ligands. The trans-influence dictates that the sulfur atoms are trans to the nitrogen atoms.

3.4 NLO test

The NLO efficiency of ACCTC crystal was evaluated by the Kurtz and Perry powder technique using a Q-switched mode locked Nd^{3+}:YAG laser emitting 1.064 μm, 8-ns laser pulses with spot radius of 1 mm. The input laser beam was passed through an IR reflector and then directed on the powdered sample of ACCTC. The light emitted by the sample was measured by the photo-diode detector and oscilloscope assembly. Microcrystalline materials of KDP and urea were used for comparison with ACCTC while performing the SHG study. All the samples were made of similar grain size of about 150 micrometers before subjecting them into experimental part. For a laser input pulse of 2.48 mJ, the second-harmonic signals 22, 130, and 46 mW were obtained through KDP, urea, and ACCTC samples, respectively. Hence, it is observed that the SHG efficiency of ACCTC is about 2 times superior to KDP. As far as the structure of ACCTC is concerned, the monomeric cation $[18C6(NH_4)^+]$ leads to the parallel alignment of the anionic zig-zag $[Cd(SCN)_3]$ chains (as shown in Fig. 3). In such parallel alignment, dipole moment from the individual chains gets added, and thereby, macroscopic SHG property is increased [22]. Hence, it is evident that the

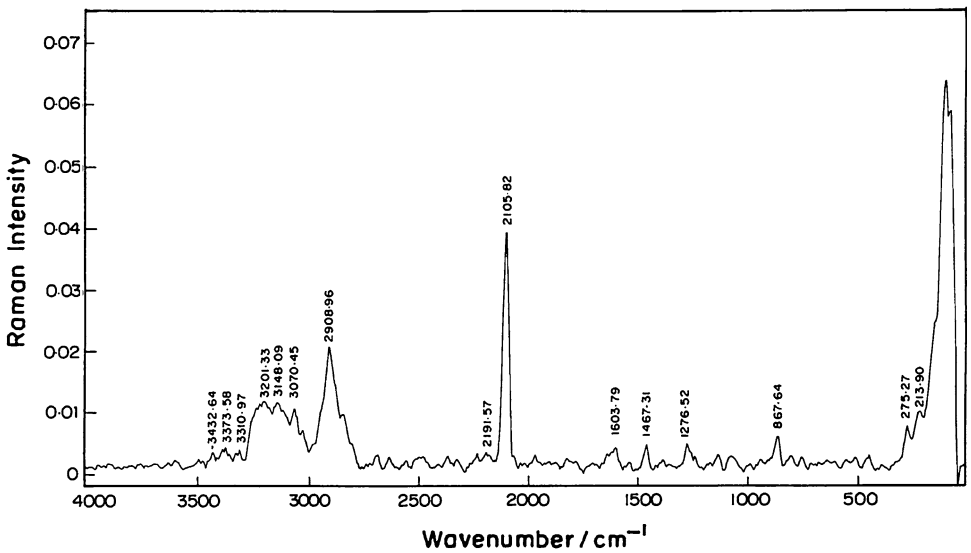

Fig. 9 FT-Raman spectrum of ACCTC

Table 3 Selected FT-Raman spectral assignments of ACCTC

Assignments	Wavenumber (cm^{-1}) ACCTC
NH stretching vibrations	3201.33, 3148.09, 3070.45
CN stretching of SCN	2105.82
CH_2 stretching vibration	1467.31
Asymmetric C–O–C stretching	1105.4
Symmetric C–O–C stretching	951.3
Twice NCS bending vibrations	867.64
CS stretching of SCN	753.4
NCS bending vibrations	457.0
CdS bending vibrations	275.27, 213.90
Lattice vibration modes	105.00, 80.94

noncentrosymmetric space group crystal (ACCTC) with parallel alignment of the anionic chains exhibits efficient second order nonlinear optical response. The SHG efficiency of similar category of IPOS series of compounds are listed in Table 4.

3.5 Optical studies

The optical transmission spectrum of the grown crystal of ACCTC was recorded using VARIAN CARY 5E spectrophotometer with the range of 200–2,500 nm and is shown in Fig. 10. A good quality ACCTC crystal of size 2 mm × 3 mm was selected and mounted in the solid sample holder and mounted in the instrument, and consequently, the transmission spectrum was recorded. The spectrum shows 80 % transmission from 200 to 345 nm and about 78 % from 345 to 998 nm. In addition, the sample shows 100 % transmission from 1,000 to 1,780 nm. Then, the percentage of transmission decreases and reaches

Table 4 SHG efficiency of ACCTC in comparison with different IPOS series crystalline compounds

IPOS series crystalline compound	SHG in terms of KDP
$[Et_4N][Cd(SCN)_3]$	1.5 [21]
$[Et_4N][Cd(SeCN)_3]$	3.0 [21]
[(18C6)Li][$Cd(SCN)_3$]	2.0 [23]
$(NH_4)[Cd(NCS)_3]\cdot C_{12}H_{24}O_6$	2.0 [Present work]

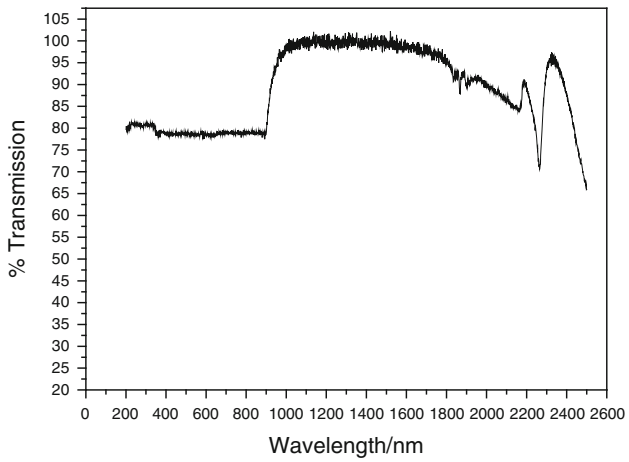

Fig. 10 UV–Vis–NIR transmission spectrum of ACCTC

65 % at 2,500 nm with an absorption peak at about 2,300 nm. Hence, it is evident that the sample possesses wide transparency window from 200 to 2,500 nm. Similar result was obtained in the IPOS series hybrid compound [(18C6)K][$Cd(SCN)_3$], which shows transparency from 220 to 3,300 nm [22]. This broader transparency window (ultraviolet to IR) attests the usefulness of this material for SHG and other optoelectronic applications.

3.6 Thermal studies

The TG-DSC analysis of ACCTC was carried out using SDT Q600 V20.9 thermal analyzer instrument in the temperature range 30–1,000 °C at a heating rate of 10 K/min (Fig. 11). The experiment was performed in a nitrogen atmosphere. The TG curve of ACCTC shows the decomposition of the ACCTC sample at various temperatures. The DSC profile shows that the sample is stable up to 237.92 °C as there is no phase change between the room temperature and 237.92 °C. It also evidences the absence of water molecules in the ACCTC sample. The first stage of decomposition in TG curve is a overlapping stage in which the breakdown of $[(NH_4)[Cd(NCS)_3]\cdot C_{12}H_{24}O_6]$ into 18C6, NH_4SCN and $Cd(SCN)_2$ may happen. Further, loss of 18-crown-6-ether molecule (48 %) and NH_4SCN (13 %) may take place successively in the first stage itself whose theoretical total value (47.00 % + 13.38 % = 60.38 %) is comparable with the experimentally observed weight loss (61.0 %). This fact clearly shows that there is only one 18-crown-6-ether molecule in the ACCTC crystalline compound, and further, the ammonium thiocyanate may decompose into the fragments such as ammonia (NH_3), carbon bisulfide (CS_2), and hydrogen sulfide (H_2S). The decomposition of 18C6 and NH_4SCN was confirmed by the peaks 237.92 °C and 328.40 °C observed in the DSC profile. During the second stage, the breakdown of $Cd(SCN)_2$ may occur, and the corresponding metal sulfides, nitrogen gas, and dicyanogen may be released out. The final product may be CdS whose weight percentage (24 %) is comparable with its theoretical value (25 %). Thermal analysis revealed that the sample is thermally stable up to 237.92 °C, which is comparatively far better than the thermal stability of the other well-known IPOS series compound $[(18C6)Li][Cd(SCN)_3]$ (CLTC) (170 °C) [24] and bi-metal-thiocyanate compounds such as $[Hg(N_2H_4CS)_4Mn(SCN)_4]$ (TMTM) (199.06 °C) [29] and $[Hg(N_2H_4CS)_4Zn(SCN)_4]$ (TMTZ) (185 °C) [30], respectively.

4 Conclusion

This paper reports the growth of high-quality single crystals of $[(NH_4)[Cd(NCS)_3]\cdot C_{12}H_{24}O_6]$ by slow evaporation technique for the first time. The cell parameters of grown crystal were confirmed single crystal XRD, which reveal that the ACCTC compound crystallizes in a space group $Cmc2_1$ with cell parameters $a = 14.7568$ Å, $b = 15.4378$ Å, $c = 10.6383$ Å, $V = 2423.54$ (18) Å^3, and $Z = 4$. The solubility of ACCTC was estimated for different temperatures, and it indicates the low solubility in water. The functional groups of 18-crown-6-ether, thiocyanate, and optical transparency of ACCTC crystal were analyzed. Interestingly, ACCTC is optically transparent in the entire ultraviolet, visible, and IR region (200–2,500 nm with an absorption peak at about 2,300 nm). The TG-DSC thermal analysis revealed that the sample is thermally stable up to 237.92 °C, which is comparatively far better than the thermal stability of CLTC (170 °C). The SHG efficiency of the sample is found to be twice that of KDP. The preliminary investigations of ACCTC sample show

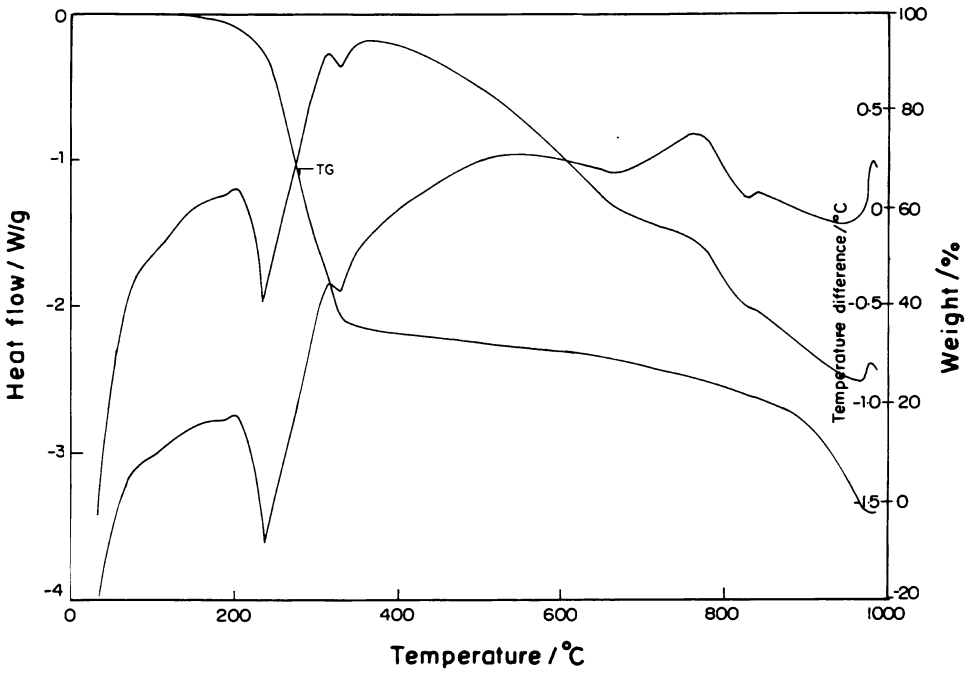

Fig. 11 TG-DSC traces of ACCTC

that the sample is one of the candidate materials suitable for NLO applications.

Acknowledgments One of the authors (K. R) thanks University Grants Commission (UGC), New Delhi for funding this research project (F. No. 41-1008/2012 (SR)). The authors also thank Dr. P. K. Das (Indian Institute of Science, Banglore), Dr. Babu Varghese (Sophisticated Analytical Instrument Facility, IIT Madras), Mr. S. Ramasamy (Central Instrumentation facility, Pondicherry University) for extending their research facilities. The authors wholeheartedly thank Dr. M. Nizam Mohideen (Department of Physics, New College, Chennai) for his help and encouragement.

References

1. H. Zhang, X. Wang, B.K. Teo, J. Am. Chem. Soc. **118**, 11813 (1996)
2. K.E. Schwiebert, D.N. Chin, J.C. MacDonald, G.M. Whitesides, J. Am. Chem. Soc. **118**, 4018 (1996)
3. H. Zhang, X. Wang, H. Zhu, W. Xiao, B.K. Teo, J. Am. Chem. Soc. **119**, 5463 (1997)
4. H. Zhang, X. Wang, K. Zhang, B.K. Teo, Inorg. Chem. **37**, 3490 (1998)
5. S. Khodia, D. Josse, J. Zyss, J. Opt. Soc. Am. B **15**, 751 (1998)
6. S. Guo, D. Xu, L. Mengkai, D. Yuan, Z. Yang, G. Zhang, S. Sun, X.Q. Wang, M. Zhou, M. Jiang, P. Yang, W. Yu, Prog. Cryst. Growth Charact. Mater. **111**, 114 (2000)
7. M. Zhou, W.T. Yu, D. Xu, S.Y. Guo, M.K. Lu, D.R. Yuan, Z. Kristallogr. NCS **215**, 425 (2000)
8. A. Mosset, B.B. Muriel, A. Lecchi, R. Masse, J. Zaccaro, Solid State Sci. **827**, 834 (2002)
9. I.E. Szczygie, Z. Jagoda, J. Kiak, M. Korabik, J. Therm. Anal. Calorim. **677**, 684 (2012)
10. I. Vetha Potheher, K. Rajarajan, R. Jeyasekaran, M. Vimalan, F. Yogam, P. Sagayaraj, J. Therm. Anal. Calorim. (2012) (Article in press)
11. I. Vetha Potheher, K. Rajarajan, M. Vimalan, S. Tamilselvan, R. Jeyasekaran, P. Sagayaraj, Phys. B **406**, 3210 (2011)
12. K. Rajarajan, G. Mani, I. Vetha Potheher, G.M. Joe Jesudurai, M. Vimalan, D. Christy, J. Madhavan, P. Sagayaraj, J. Phys. Chem. Solids **68**, 2370 (2007)
13. K. Rajarajan, G.P. Joseph, S.M. Ravi Kumar, I. Vetha Potheher, A. Joseph Arul Pragasam, K. Ambujam, P. Sagayaraj, Mater. Manuf. Process. **22**, 370 (2007)
14. I. Vetha Potheher, K. Rajarajan, S. Nagaraja, P. Sagayaraj, J. Cryst. Growth **310**, 124 (2008)
15. A. Gacemi, D. Benbertal, B.B. Muriel, A. Lecchi, A. Mosset, Z. Anorg. Allg. Chem. **629**, 2516 (2003)
16. X.T. Liu, X.Q. Wang, X.J. Lin, G.H. Sun, G.H. Zhang, D. Xu, Appl. Phys. A **107**, 949 (2012)
17. K. Rajarajan, P.C. Thomas, I. Vetha Potheher, G.P. Joseph, S.M. Ravi Kumar, S. Selvakumar, P. Sagayaraj, J. Cryst. Growth **304**, 435 (2007)
18. V.R. Thalladi, S. Brasselet, H. Weiss, D. Bleser, A.K. Katz, H.L. Carrell, R. Boese, J. Zyss, A. Nangia, G.R. Desiraju, J. Am. Chem. Soc. **120**, 2563 (1998)
19. H. Zhang, X. Wang, H. Zhu, W. Xiao, B.K. Teo, Inorg. Chem. **38**, 886 (1999)
20. H. Zhang, X. Wang, K. Zhang, B.K. Teo, Coord. Chem. Rev. **183**, 157 (1999)
21. H. Zhang, D.E. Zelmon, G.E. Price, B.K. Teo, Inorg. Chem. **39**, 1868 (2000)
22. H. Zhang, D.E. Zelmon, J. Cryst. Growth **234**, 529 (2002)
23. J.J. Zhang, X. Shu, Spect. Chimi. Acta Part A Mole. Biomole. Spect. **74**, 532 (2009)
24. J.J. Zhang, Y. Huang, Cryst. Res. Technol. **44**, 985 (2009)
25. V. Ramesh, K. Rajarajan, K. Sendil Kumar, A. Subashini, M. Nizam Mohideen, Acta Cryst. Sec. E **E68**, m335 (2012)
26. G. Yang, W. Leng, Y. Zhang, Z. Chen, J.V. Houten, Polyhedron **18**, 1273 (1999)
27. D. Alok, A.D. Bokare, A. Patnaik, Cryst. Res. Technol. **36**, 465 (2004)
28. A.N. Chekhlov, Russ. J. Inorg. Chem. **50**, 541 (2005)
29. K. Rajarajan, P.C. Thomas, I. Vetha Potheher, G.P. Joseph, S.M. Ravi Kumar, S. Selvakumar, P. Sagayaraj, J. Cryst. Growth **304**, 435 (2007)
30. X.Q. Wang, D. Xu, X. Cheng, J.J. Huang, Cryst. Growth **271**, 120 (2004)